

Impact of glutaraldehyde cross-linking on the advanced platelet-rich fibrin membrane: Macroscopic, conventional light microscopic and scanning electron microscopic analysis

Gayathri Gunjiganur Vemanaradhya^{A–F}, Sartaz Rahman^{B,D}, Deepika Mani Adi^{B,D}, Laxmi Machetty^{C,E}

Department of Periodontology, Bapuji Dental College and Hospital, Davangere, India

A – research concept and design; B – collection and/or assembly of data; C – data analysis and interpretation;
D – writing the article; E – critical revision of the article; F – final approval of the article

Dental and Medical Problems, ISSN 1644-387X (print), ISSN 2300-9020 (online)

Dent Med Probl. 2023;60(1):79–86

Address for correspondence

Gayathri Gunjiganur Vemanaradhya
E-mail: gayathri_dental@rediffmail.com

Funding sources

None declared

Conflict of interest

None declared

Acknowledgements

We would like to thank Prof. Ahmed Mujib Bangalore Rahim and Dr Neetu Telagi from the Department of Oral Pathology and Oral Histology of the Bapuji Dental College and Hospital, Davangere, India, for macroscopic and light microscopic analysis, Mr. Jadav Maruthi from Osmania University, Hyderabad, India, for the SEM examination, and Dr. Usha Govindaroy Venkatesh from the Department of Public Health Dentistry of the Bapuji Dental College and Hospital, Davangere, India, for carrying out the statistical analysis.

Received on September 22, 2021

Reviewed on January 15, 2022

Accepted on January 31, 2022

Published online on March 29, 2023

Cite as

Gunjiganur Vemanaradhya G, Rahman S, Adi DM, Machetty L. Impact of glutaraldehyde cross-linking on the advanced platelet-rich fibrin membrane: Macroscopic, conventional light microscopic and scanning electron microscopic analysis. *Dent Med Probl.* 2023;60(1):79–86. doi:10.17219/dmp/146271

DOI

10.17219/dmp/146271

Copyright

Copyright by Author(s)

This is an article distributed under the terms of the Creative Commons Attribution 3.0 Unported License (CC BY 3.0) (<https://creativecommons.org/licenses/by/3.0/>).

Abstract

Background. Advanced platelet-rich fibrin (A-PRF) is a biopolymer that releases growth factors to facilitate healing. Along with other barrier membranes, the A-PRF membrane has proven to be beneficial in guided tissue regeneration (GTR) treatment. The cross-linking of the A-PRF membrane with glutaraldehyde (GLUT) has been attempted previously, and has been shown to prolong its degradation time and improve its mechanical properties. In the present study, the effects of GLUT cross-linking on macroscopic changes in the A-PRF membrane were assessed, and microscopic features were analyzed using a light microscope and a scanning electron microscope (SEM).

Objectives. The aim of the present study was to evaluate and compare the effects of GLUT cross-linking on the A-PRF membrane through the macroscopic, microscopic and SEM examinations.

Material and methods. A total of 18 human A-PRF membrane samples were prepared, half of which were treated with 0.1% GLUT, and the remaining were left untreated. The macroscopic measurements of the samples included weight, length and thickness, while specimen slides were prepared for light microscopic evaluation and SEM analysis.

Results. The GLUT cross-linked membranes weighed more and were thicker than the non-cross-linked membranes, but there was no change in length. Light microscopic images showed fewer cells at the head and tail, though cells were abundant in the body of the A-PRF membrane. The images acquired using SEM showed fibrin strands of greater thickness, but fewer interspersed cell bodies in the cross-linked membranes.

Conclusions. This in vitro study revealed an increase in thickness and cross-linking fiber density along with the presence of viable cells in the GLUT-treated A-PRF membrane, which may prove its effectiveness in healing or serving as a barrier membrane in clinical trials.

Keywords: glutaraldehyde, advanced platelet-rich fibrin, cross-linking

Introduction

Advanced platelet-rich fibrin (A-PRF) is a second-generation, self-clotting, platelet-concentrated, blood-derived biomaterial rich in white blood cells. The material is prepared through the contact activation of intrinsic coagulation pathways, using low-speed centrifugation, without the need for additional coagulation factors.¹ It provides the sustained release of high concentrations of growth factors, which enhance collagen synthesis and supplement progenitor cells.² Studies have demonstrated the use of PRF membranes in the treatment of periodontal osseous defects with open-flap debridement³ to cover the defects filled with bone grafts, potentially also functioning as a guided tissue regeneration (GTR) membrane.⁴ Furthermore, PRF has been used as an adjunct to GTR membranes to facilitate vascularization, to guide the migration of epithelial cells, and to provide growth factors to enhance soft and hard tissue regeneration.⁵ A retrospective clinical trial revealed promising bone gain associated with the guided bone regeneration (GBR) procedure, which included combining membranes, bone grafts and PRF for vertical and horizontal bone augmentation.⁶ However, the major shortcomings of PRF include its rapid degradability and poor mechanical strength. Thus, the use of PRF membranes on their own has not proven to be popular in GTR treatment, as they cannot maintain space for tissue regeneration or prevent the migration of epithelial cells for a sufficient period of time.⁵ Fortunately, biopolymers can be modified to achieve an ideal combination of mechanical properties, geometry and surface chemistry by subjecting them to cross-linking treatment.⁷ Therefore, overcoming the shortcomings of PRF membranes would allow clinicians to use them successfully in GBR and GTR therapies.

The 2 aldehyde groups of glutaraldehyde (GLUT) can react with free amino groups of polypeptide chains to form Schiff bases, which leads to the cross-linking of biological tissue materials.⁸ A 0.1% cross-linked amniotic membrane had the maximum cross-linking of its amino groups, resulting in a significant increase in thermal stability and an increased degradation time.⁹ Furthermore, no morphological abnormalities and good cell viability were observed at low concentrations.⁹ In addition, GLUT vapor treatment was used to maintain the bioactivity of the electrospun fibrinogen scaffolds.¹⁰

The toxicity of GLUT is related to its concentration, the duration of cross-linking and its release from the cross-linked material. The exposure of cell cultures to 0.1% GLUT cross-linked amniotic membranes for 24 h led to a significant decrease in the number of viable corneal epithelial cells as compared to the groups exposed to lower concentrations.⁹ Gelatin films cross-linked with a 0.1% GLUT solution for 24 h released 2 wt% after 1 week, which increased up to 9 wt% after 4 weeks.¹¹ In our previous study, A-PRF membranes cross-linked with 0.1% GLUT

for 10 min showed an increased mechanical strength and a prolonged degradation time, and a 0.083 wt% GLUT release after 24 h, with no further release over the following 2 weeks.¹²

Previous results have opened up the possibility of using GLUT cross-linked A-PRF as an efficient GTR membrane. However, its ultrastructure requires extensive evaluation before it can be used as a clinical application in periodontal regeneration. Therefore, this study aimed to evaluate and compare the macroscopic parameters, light microscope-acquired images and scanning electron microscope (SEM)-acquired images of GLUT cross-linked A-PRF membranes and non-cross-linked A-PRF membranes.

Material and methods

Nine systemically healthy male volunteers, aged 20–35 years, were selected from the outpatient department of the Bapuji Dental College and Hospital, Davangere, India. Volunteers who smoked tobacco products or who were receiving anticoagulant therapy were excluded. The study design and consent forms for all the procedures performed on human subjects were approved by the board of the institutional Ethical Committee (No. BDC/Exam/509/2019-20). The purpose of the study was verbally explained to the volunteers, and written consent to participate in the study was obtained before its commencement. Blood was drawn from each volunteer (20 mL) to prepare 2 A-PRF membranes.

Preparation of advanced platelet-rich fibrin clots

The A-PRF samples were prepared according to the protocol developed by Ghanaati et al.¹³ Venous blood (20 mL) was collected via the cubital vein, using Vacutainer™ tubes (Becton Dickinson Company, Tokyo Japan), and transferred to A-PRF tubes (Zhejiang Gongdong Medical Technology Co., Ltd., Taizhou, China). The A-PRF tubes were immediately centrifuged at 1,500 rpm for 14 min, using the A-PRF12 system (Dragon Laboratory Instruments Ltd., Beijing, China). Centrifugation led to the formation of 3 separate layers, including a red blood cell (RBC) base, an acellular plasma supernatant (platelet-poor plasma – PPF) and a PRF clot in the middle. The clot was separated from the A-PRF tube and the membrane was prepared by compression in an A-PRF expression box, which maintained a uniform size and a standard thickness of 1 mm for each clot. The prepared membranes were divided into experimental and control samples, and immediately subjected to the required treatment for macroscopic and microscopic evaluation to avoid the loss of functional capacity and cell integration due to a prolonged bench time.¹⁴

Glutaraldehyde cross-linking of platelet-rich fibrin

A total of 18 A-PRF membranes were prepared, out of which 9 membranes were cross-linked with 10 mL of a 0.1% GLUT solution in phosphate-buffered saline (PBS) at a pH of 7.4 for 10 min at room temperature. The remaining 9 non-cross-linked membranes were used as control samples.¹² Macroscopic evaluation, and light microscopy and SEM imaging were performed in triplicate to avoid bias.

Macroscopic analysis

The length and weight of A-PRF membranes were measured using a ruler and a digital balance (Contech Instruments Limited, Mumbai, India), respectively, as shown in Fig. 1A and 1B. Both the experimental and control samples were placed on a pre-weighed sterile microscope slide for weight and length measurements.

Light microscopic analysis

The ultrastructure of fibrin and the distribution of cell bodies within the A-PRF membranes were examined using the Olympus CX21i light microscope (Olympus, New Delhi, India). Before analysis, the A-PRF membranes were fixed in 10% neutral buffered formalin for 24 h at room temperature for paraffin inclusion.¹⁵ The membranes were stored on a microscope slide during fixation to avoid distortion. Successive sections (4-micrometer-thick) were collected along the center of the long axis of the membranes and stained with hematoxylin and eosin (H&E). Each section was divided into 3 areas of equal size, including head/face (proximal), body (center) and tail (distal), as shown in Fig 1C. The center of each area was observed to analyze the distribution of visible cell bodies (marked in dark purple) under $\times 100$, $\times 200$ and $\times 400$ magnification. For semi-quantitative evaluation, manual cell body

counting was performed at $\times 200$ magnification by an oral pathologist. The total number of cell bodies counted was used to compare the distribution among the 3 areas of the membrane.¹⁶ Most of the cells were concentrated in the body area.

Scanning electron microscopic analysis

The surface microstructure, topography, morphology, and compositional information of the A-PRF membranes were examined using the FE-SEM SU6600 (Hitachi High Technologies America, Inc., Hillsboro, USA). Before analysis, The samples were dehydrated by passing each specimen through a series of graded ethanol-water mixtures, and then dried by the critical point method. After drying, the samples were sputter-coated with gold and examined under SEM.¹⁷ Images were acquired using magnifications ranging from 2.5 kX to 10 kX.

Statistical analysis

The macroscopic and microscopic (semi-quantitative) evaluation values were tabulated and subjected to statistical analysis. Comparisons were made between the cross-linked and control samples using Student's independent *t* test. Values of $p < 0.001$, $p < 0.05$ and $p > 0.05$ were considered highly significant, significant and non-significant, respectively.

Results

Macroscopic analysis

A significant weight increase was recorded in the GLUT cross-linked samples as compared to the non-cross-linked controls ($p = 0.010$). Meanwhile, the lengths of both the experimental and control samples were almost identical, and were not found to be significantly different ($p = 0.100$) (Table 1).

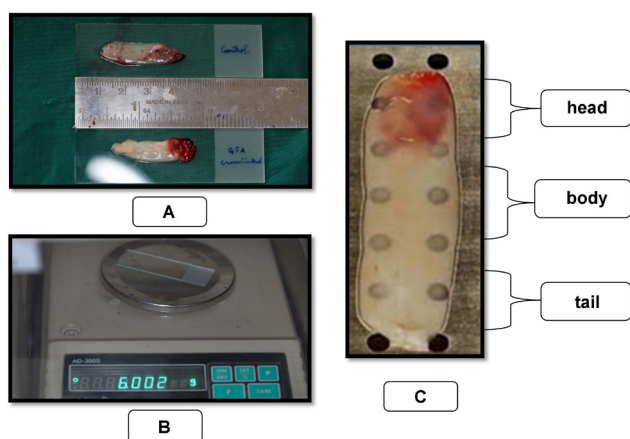


Fig. 1. A, B – evaluation of macroscopic parameters; C – light microscopy procedure

Table 1. Comparison of macroscopic parameters between the test and control groups

Parameter	Group	<i>n</i>	<i>M</i> \pm <i>SD</i>	<i>SEM</i>	95% <i>CI</i>	<i>p</i> -value
Weight [g]	test	3	0.32 \pm 0.15	0.008	0.01–0.07	0.010*
	control	3	0.28 \pm 0.10	0.005		
Length [cm]	test	3	3.43 \pm 0.05	0.033	0.03–0.23	0.100
	control	3	3.33 \pm 0.05	0.033		

Test group: glutaraldehyde (GLUT) cross-linked advanced platelet-rich fibrin (A-PRF) membranes. Control group: Non-cross-linked A-PRF membranes. *M* – mean; *SD* – standard deviation; *SEM* – standard error of the mean; *CI* – confidence interval; * statistically significant ($p < 0.05$).

Light microscopic analysis

Due to the H&E stain, the nuclei of the cell bodies stained a dark purple. Erythrocytes and the cytoplasm of the cell bodies were reddish pink or dark pink. Meanwhile, the fibrin network appeared light pink.

Head/face

The clusters of erythrocytes and residual cell bodies could be observed entrapped within the fibrin network in both the experimental and control samples. In addition, the fibrin network was denser in the experimental samples, and there were significantly fewer cell bodies in the experimental samples than in the control ones ($p = 0.002$) (Fig. 2, Table 2).

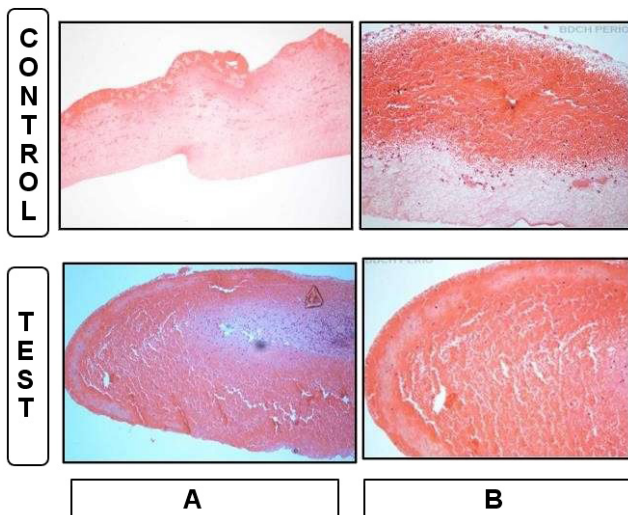


Fig. 2. Microscopic pictures of the head/face of the advanced platelet-rich fibrin (A-PRF) membrane samples of the control and test groups

A – $\times 100$ magnification; B – $\times 200$ magnification.

Table 2. Comparison of cellular body distribution between the test and control groups

Parameter	Group	n	$M \pm SD$	SEM	95% CI	p-value
Head	test	3	148.30 ± 7.63	4.40	–60.6 to –26.0	0.002*
	control	3	191.60 ± 7.63	4.40		
Body	test	3	316.60 ± 76.30	44.09	–597.5 to –335.7	0.001**
	control	3	783.30 ± 28.80	16.66		
Tail	test	3	58.30 ± 7.63	4.40	–40.6 to –6.0	0.020*
	control	3	81.60 ± 7.63	4.40		

* statistically significant ($p < 0.05$); ** highly statistically significant ($p < 0.001$).

Body

The vast majority of cell bodies (95%) were present in the body of the A-PRF membranes, and a mature fibrin network, as well as cellular components, were well separated from each other in both the experimental and control samples. Most of the cell bodies observed were lymphocytes and plasma cells, particularly those entrapped within the fibrin network. The clusters of erythrocytes were interspersed between cell bodies in the control group. In the experimental group, cellular components were separated by fibrillar bands. Furthermore, the fibrin network was abundant between cells, and there was a significantly lower cell density in the experimental samples as compared to the control samples ($p = 0.001$). Cells appeared intact and had a normal shape in both the experimental and control samples (Fig. 3, Table 2).

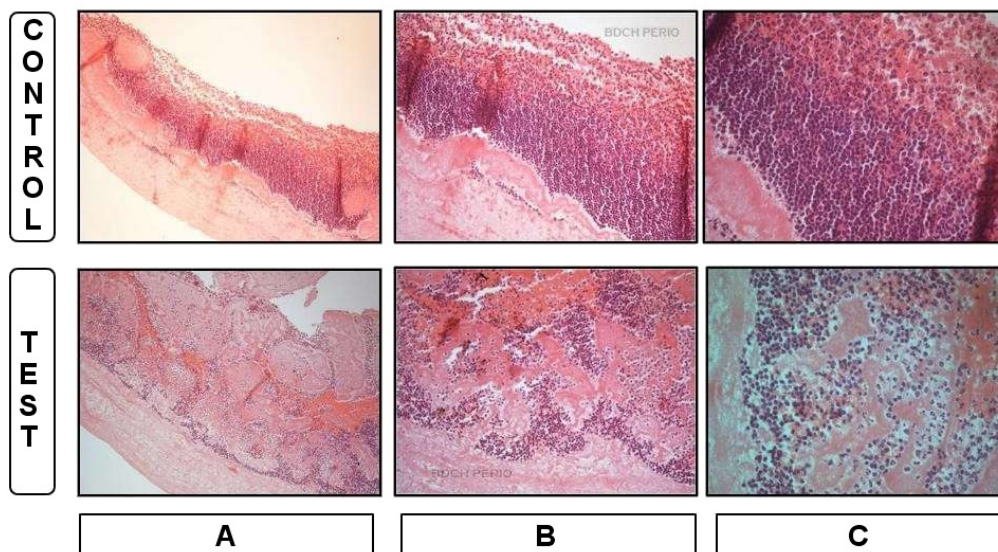


Fig. 3. Microscopic pictures of the body of the advanced platelet-rich fibrin (A-PRF) membrane samples of the control and test groups

A – $\times 100$ magnification; B – $\times 200$ magnification; C – $\times 400$ magnification.

Tail

The tail of the membrane was bordered by a homogeneous well-organized fibrin mesh structure with continuous integrity, which enclosed the clusters of erythrocytes in both the experimental and control samples. In addition, residual cell bodies were entrapped within the fibrin network and between the clusters of erythrocytes. Loosely arranged fibers and a textured fibrin network were visible in the experimental samples, while the control group had a fibrin network of densely organized parallel strands. The number of cells was significantly higher in the control group than in the experimental group ($p = 0.020$) (Fig. 4, Table 2).

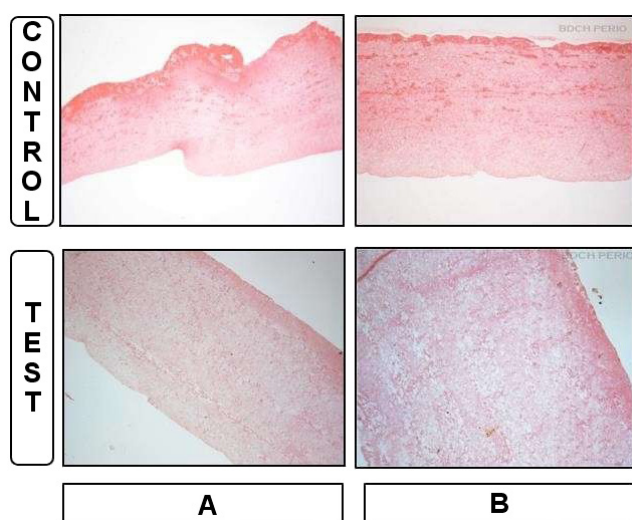


Fig. 4. Microscopic pictures of the tail of the advanced platelet-rich fibrin (A-PRF) membrane samples of the control and test groups

A – $\times 100$ magnification; B – $\times 200$ magnification.

Scanning electron microscopic analysis

The SEM analysis provided information on the surface topography, fibrin network, cell content, and internal structure of each membrane within a small area of great depth. At a low magnification of 2.5 kX, the control samples had a highly irregular surface with overlying spherical structures, which were identified as leukocytes. A dense aggregate of platelets resting on a mature fibrin background was also observed. Platelet morphology appeared to be modified by the aggregation and clotting process. The experimental samples had a dense fibrin matrix with surface morphology similar to that of medical gauze and had fewer cellular components as compared to the control samples.

At a higher magnification of 10 kX, a continuous dense fibrin network with entrapped cellular structures was observed in the control samples. Meanwhile, a thick fibrin fiber network of a porous structure was observed in the experimental samples, where intact leukocytes and platelets were found to be entrapped (Fig. 5).

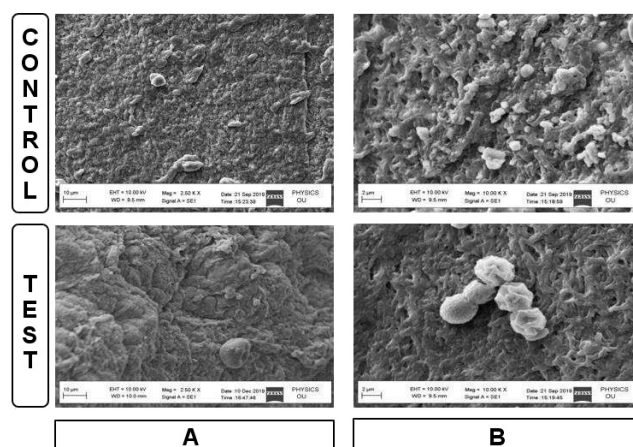


Fig. 5. Scanning electron microscopy (SEM) pictures of the advanced platelet-rich fibrin (A-PRF) membrane samples of the control and test groups
A – 2.5 kX magnification; B – 10 kX magnification.

Discussion

The concentration of RBC tends to decrease in elderly patients, which makes it easier to separate the plasma layers and a larger modified A-PRF clot can be produced as compared to younger patients. The PRF membranes produced from female patients tend to be 17% larger than those produced from male patients due to reduced RBC concentration and hematocrit levels in peripheral blood.¹⁸ Although the platelet concentration is higher in females than males, females show cyclical variations. Indeed, the platelet concentration appears to align with the estrogen levels and reduces before the onset of menstruation, before peaking at the follicular and luteal phases.¹⁹ Low platelet and leukocyte counts were observed in tobacco smokers due to alterations in various hematological parameters.²⁰ Meanwhile, female smokers reach menopause early, which leads to reduced platelet activation and a higher mean platelet count due to falling estrogen levels.²¹ In diabetic patients, osmotic effects, an increase in the glucose levels and the presence of glucose metabolites in blood lead to higher levels of larger and more reactive platelets.²² In addition, patients undergoing anticoagulant therapy experience a delay in coagulation cascade activity, which adversely affects fibrin clot formation.²³ To avoid bias, all the volunteers included in this study were males, young, non-smokers, systemically healthy, and not receiving anticoagulant therapy.

Modifications to the PRF preparation procedure by adopting the low-speed centrifugation concept (LSCC), a process that employs low G-forces, led to the development of A-PRF. In comparison with standard PRF (S-PRF), the LSCC process results in enhanced neutrophilic granulocytes, which contribute to the differentiation of monocytes into macrophages, an increase in the cytokine levels, higher growth factor concentrations, and an increased release bone morphogenetic proteins. Such improvement leads to earlier vascularization, and more rapid soft and

hard tissue regeneration.¹³ Injectable PRF (i-PRF) is also prepared using LSCC, and has higher growth factor levels and increased anti-inflammatory efficacy; however, it is a liquid and flowable form of PRF, which is used either alone or in combination with other biomaterials.²⁴

In its membranous form, A-PRF can be placed on surgical wounds for healing purposes, as it acts as a fibrin glue due to its adhesive mechanical properties and biological functions.² It has been shown *in vitro* that fibrin membranes may be better scaffolds for the proliferation of periosteal and osseous cells than collagen membranes.²⁵ Therefore, a previously published study examined the mechanical properties and degradation time of GLUT cross-linked membranes with the intention of using them as a more viable and cost-effective barrier membrane and scaffold for periodontal regeneration.¹²

Glutaraldehyde is one of the most commonly used cross-linking agents. Perpetuated exposure to a high concentration of GLUT leads to incomplete cross-linking due to rapid initial polymerization at the surface of the fibers. This prevents GLUT from accessing molecules within the deeper areas of the fibrin structure for the initiation of cross-linking by the creation of nucleation sites or a static hindrance, which leads to the consumption of large amounts of free GLUT and subsequent high toxicity.²⁶ Amniotic membrane matrices treated with low-concentration GLUT displayed good compatibility with human corneal epithelial cells.⁹ As such, the A-PRF membranes obtained in this study were treated with 0.1% GLUT for 10 min to achieve membrane cross-linking without toxic effects. Indeed, only minimal GLUT was released after 24 h, and no further release was observed over the following 2 weeks.¹²

In this study, an increase in the weight of the GLUT cross-linked samples was observed, which could be attributed to the penetration of GLUT into the membrane. Glutaraldehyde primarily fixes the surface of the fibrin fibers to create a polymeric network and initiate cross-linking. Therefore, GLUT cross-linking increases the molecular weight of proteins and alters their conformation.²⁶ No change was observed in the membrane length between the experimental and control groups following GLUT cross-linking. However, a shrinkage of A-PRF membranes was observed when they were subjected to heat compression at 90°C and 120°C for 15 s and 2 s, respectively.²⁷

Due to higher centrifugal force, platelets and inflammatory cells within the fibrin scaffold were observed mainly in the proximal portion. The LSCC used to produce A-PRF membranes adopts low G-forces to reduce cell pull-down, which increases the number of leukocytes trapped within the fibrin matrix of the top layer.¹³ Also, the top layer at the center of the membrane may have been stabilized when the clot was pressurized in the PRF box, which may explain the denser distribution of cells in the body of the experimental and control membranes. The reduced centrifugal force used for A-PRF preparation

caused lower leukocyte infiltration into the RBC fraction, meaning more were present in the adjacent fibrin clot, although the RBC fraction was not eliminated.¹³ As a result, more leukocytes were found at the center, and erythrocyte clusters were observed in the head and tail of the A-PRF membrane under the light microscope. However, this is in contrast to other studies, which showed a greater concentration of cell bodies in the head of the membrane and homogenous platelet aggregate distribution in the tail of the membrane.^{15,16} Such differences may be due to variations in the equipment and materials used, such as the centrifuge and tubes, and variations in the protocols, such as the tube temperature, the rpm rate, gravitational force, or the duration of centrifugation.¹⁶

The fibrin network of the GLUT-treated A-PRF membranes was slightly thick and loose, and had a reticular arrangement, which was in contrast to the control samples. The presence of such thick fibrin fibers and high serum retention within its spaces could enhance the volume-to-surface area ratio, and may give GLUT cross-linked membranes an advantage over normal A-PRF membranes in relation to their degradation rate.¹² In the tails of the experimental and control membranes, fibrin strands were condensed and adhered to each other, which may have been due to the compression of the fibrin matrix during membrane preparation.¹⁵

The thick, dense and regular pattern found in the fibrin network of the experimental samples is supported by the results of a previous study, where increased tensile strength and toughness were observed in GLUT cross-linked A-PRF membranes.¹² The SEM analysis also revealed greater porosity in the GLUT-treated membranes, which might facilitate cell migration and the release of growth factors, both of which are important attributes of a biological healing matrix.¹⁷ Furthermore, the SEM analysis of the experimental membranes supports the light microscopy findings regarding a decrease in cellular components and an increase in fibrin density. In the non-cross-linked A-PRF membranes, leukocytes and platelets were well distributed and were not clumped. In addition, the control matrices had lower porosity, which is consistent with the findings of Isobe et al., who found A-PRF membranes to contain denser and more mature fibrin threads.²⁸

The SEM-acquired images revealed the presence of mutilated cells in the control membranes at a lower magnification. These damaged cells raised concerns, as they may release pro-inflammatory mediators. In this regard, the ratio of activated and preserved cells to damaged cells may play an important role in regulating the inflammatory processes clinically, which needs to be addressed in future work.¹⁶ Acceleration rates of more than 1 m/s² cause damage to cells and alter their distribution. The A-PRF centrifuge used in this study has a rate of 3 m/s²,¹⁶ which may explain the appearance of mutilated/aggregated platelets in the control membranes at lower magnification.

In the experimental group, the thick and dense fibrin matrix may have disguised these modified cells due to the focus being at a greater depth and the limited surface area coverage at a higher magnification.

The microscopic (light microscope/SEM) evaluations of A-PRF membranes are scarce,^{15,17} and most studies have used conventional microscopy, which requires the dehydration or drying of specimens. Such preparation processes may cause topographical, morphological and compositional changes to the cells and fibers of A-PRF membranes. Therefore, future research using environmental SEM,²⁹ or with modifications to conventional SEM by using the wet cover method³⁰ will allow the observation of wet specimens and may overcome the limitations of conventional SEM.

Conclusions

The present descriptive in vitro study throws light on the possibility of using GLUT-treated A-PRF as a GTR membrane. It reaffirms the impact of GLUT as a cross-linking agent in the production of a resilient and viable biological membrane. However, the research is still at a primitive stage. Further evaluation of the cytotoxic effects and compatibility with viable regenerative cells is required before its clinical application in the field of periodontal regeneration.

Ethics approval and consent to participate

The study design and consent forms for all the procedures performed on human subjects were approved by the board of the institutional Ethical Committee at the Bapuji Dental College and Hospital, Davangere, India (No. BDC/Exam/509/2019-20). The purpose of the study was verbally explained to the volunteers, and written consent to participate in the study was obtained before its commencement. The study was performed in accordance with the Declaration of Helsinki ethical standards.

Data availability


All data generated and/or analyzed during this study is included in this published article.


Consent for publication


Not applicable.


ORCID iDs

Gayathri Gunjiganur Vemanaradhya

 <https://orcid.org/0000-0002-7791-4113>

Sartaz Rahman  <https://orcid.org/0000-0001-5447-1279>

Deepika Mani Adi  <https://orcid.org/0000-0002-3126-6675>

Laxmi Machetty  <https://orcid.org/0000-0002-0775-6498>

References

1. Dohan DM, Choukroun J, Diss A, et al. Platelet-rich fibrin (PRF): A second-generation platelet concentrate. Part I: Technological concepts and evolution. *Oral Surg Oral Med Oral Pathol Oral Radiol Endod.* 2006;101(3):e37–e44. doi:10.1016/j.tripleo.2005.07.008.
2. Lei L, Yu Y, Han J, et al. Quantification of growth factors in advanced platelet-rich fibrin and concentrated growth factors and their clinical efficacy as adjunctive to the GTR procedure in periodontal intrabony defects. *J Periodontol.* 2020;91(4):462–472. doi:10.1002/JPER.19-0290
3. Vu Pham TA. Intrabony defect treatment with platelet-rich fibrin, guided tissue regeneration and open-flap debridement: A randomized controlled trial. *J Evid Based Dent Pract.* 2021;21(3):101545. doi:10.1016/j.jebdp.2021.101545.
4. Pradeep AR, Bajaj P, Rao NS, Agarwal E, Naik SB. Platelet-rich fibrin combined with a porous hydroxyapatite graft for the treatment of 3-wall intrabony defects in chronic periodontitis: A randomized controlled clinical trial. *J Periodontol.* 2017;88(12):1288–1296. doi:10.1902/jop.2012.110722
5. Panda S, Sankari M, Satpathy A, et al. Adjunctive effect of autologous platelet-rich fibrin to barrier membrane in the treatment of periodontal intrabony defects. *J Craniofac Surg.* 2016;27(3):691–696. doi:10.1097/SCS.00000000000002524
6. Amaral Valladão CA Jr., Monteiro MF, Joly JC. Guided bone regeneration in staged vertical and horizontal bone augmentation using platelet-rich fibrin associated with bone grafts: A retrospective clinical study. *Int J Implant Dent.* 2020;6(1):72. doi:10.1186/s40729-020-00266-y
7. Reddy N, Reddy R, Jiang Q. Crosslinking biopolymers for biomedical applications. *Trends Biotechnol.* 2015;33(6):362–369. doi:10.1016/j.tibtech.2015.03.008
8. Lai JY, Li YT. Evaluation of cross-linked gelatin membranes as delivery carriers for retinal sheets. *Mater Sci Eng C.* 2010;30(5):677–685. doi:10.1016/j.msec.2010.02.024
9. Lai JY. Interrelationship between cross-linking structure, molecular stability, and cytocompatibility of amniotic membranes cross-linked with glutaraldehyde of varying concentrations. *RSC Adv.* 2014;4(36):18871–18880. doi:10.1039/C4RA01930J
10. Sell SA, Francis MP, Garg K, et al. Cross-linking methods of electrospun fibrinogen scaffolds for tissue engineering applications. *Biomed Mater.* 2008;3(4):045001. doi:10.1088/1748-6041/3/4/045001
11. Bigi A, Cojazzi G, Panzavolta S, Rubini K, Roveri N. Mechanical and thermal properties of gelatin films at different degrees of glutaraldehyde crosslinking. *Biomaterials.* 2001;22(8):763–768. doi:10.1016/S0142-9612(00)00236-2
12. Rahman S, Gayathri GV, Mehta DS. Comparative evaluation of advanced platelet rich fibrin membrane with and without glutaraldehyde crosslinking – a de novo in vitro trial. *EC Dent Sci.* 2019;18(10):2328–2337. <https://vdocuments.mx/open-access-research-article-comparative-evaluation-of-a-ecde-a-pdf-a.html?page=1>. Accessed September 5, 2019.
13. Ghanaati S, Booms P, Orlowska A, et al. Advanced platelet-rich fibrin: A new concept for cell-based tissue engineering by means of inflammatory cells. *J Oral Implantol.* 2014;40(6):679–689. doi:10.1563/aaid-joi-D-14-00138
14. Rutkowski JL, Thomas JM, Bering CL, et al. Analysis of a rapid, simple, and inexpensive technique used to obtain platelet-rich plasma for use in clinical practice. *J Oral Implantol.* 2008;34(1):25–33. doi:10.1563/1548-1336(2008)34[25:AAOARS]2.0.CO;2
15. Bhatnagar A, Patil MB, Prakash S. Microscopic evaluation of the effect of low-level laser therapy on platelet-rich fibrin: A light microscopic histological study. *Indian J Oral Health Res.* 2019;5(1):6–10. doi:10.4103/ijohr.ijohr_5_19
16. Dohan Ehrenfest DM, Pinto NR, Pereda A, et al. The impact of the centrifuge characteristics and centrifugation protocols on the cells, growth factors, and fibrin architecture of a leukocyte- and platelet-rich fibrin (L-PRF) clot and membrane. *Platelets.* 2018;29(2):171–184. doi:10.1080/09537104.2017.1293812
17. Sam G, Vadakkekuttal RJ, Amol NV. In vitro evaluation of mechanical properties of platelet-rich fibrin membrane and scanning electron microscopic examination of its surface characteristics. *J Indian Soc Periodontol.* 2015;19(1):32–36. doi:10.4103/0972-124X.145821

18. Miron RJ, Dham A, Dham U, Zhang Y, Pikos MA, Sculean A. The effect of age, gender, and time between blood draw and start of centrifugation on the size outcomes of platelet-rich fibrin (PRF) membranes. *Clin Oral Investig*. 2019;23(5):2179–2185. doi:10.1007/s00784-018-2673-x
19. Chen G, Chen L, Qin X, Xie X, Li G, Xu B. Cyclic thrombocytopenia related to menstrual cycle: A case report and literature review. *Int J Clin Exp Med*. 2014;7(10):3595–3598. PMID:25419404. PMCID:PMC4238553.
20. Butkiewicz AM, Kemona-Chetnik I, Dymicka-Piekarska V, Matowicka-Karna J, Kemona H, Radziwon P. Does smoking affect thrombopoiesis and platelet activation in women and men? *Adv Med Sci*. 2006;51:123–126. PMID:17357291.
21. Yang HJ, Suh PS, Kim SJ, Lee SY. Effects of smoking on menopausal age: Results from the Korea National Health and Nutrition Examination Survey, 2007 to 2012. *J Prev Med Public Health*. 2015;48(4):216–224. doi:10.3961/jpmph.15.021
22. Demirtunc R, Duman D, Basar M, Bilgi M, Teomete M, Garip T. The relationship between glycemic control and platelet activity in type 2 diabetes mellitus. *J Diabetes Complications*. 2009;23(2):89–94. doi:10.1016/j.jdiacomp.2008.01.006
23. de Almeida Barros Mourão CF, Miron RJ, de Mello Machado RC, Ghanaati S, Alves GG, Calasans-Maia MD. Usefulness of platelet-rich fibrin as a hemostatic agent after dental extractions in patients receiving anticoagulant therapy with factor Xa inhibitors: A case series. *Oral Maxillofac Surg*. 2019;23(3):381–386. doi:10.1007/s10006-019-00769-y
24. Özsağır ZB, Tunali M. Injectable platelet-rich fibrin: A new material in medicine and dentistry. *Mucosa*. 2020;3(2):27–33. doi:10.33204/mucosa.707865
25. Gassling V, Hedderich J, Açil Y, Purcz N, Wiltfang J, Douglas T. Comparison of platelet rich fibrin and collagen as osteoblast-seeded scaffolds for bone tissue engineering applications. *Clin Oral Implants Res*. 2013;24(3):320–328. doi:10.1111/j.1600-0501.2011.02333.x
26. Cheung DT, Perelman N, Ko EC, Nimni ME. Mechanism of crosslinking of proteins by glutaraldehyde III. Reaction with collagen in tissues. *Connect Tissue Res*. 1985;13(2):109–115. doi:10.3109/03008208509152389
27. Kawase T, Kamiya M, Kobayashi M, et al. The heat-compression technique for the conversion of platelet-rich fibrin preparation to a barrier membrane with a reduced rate of biodegradation. *J Biomed Mater Res Part B Appl Biomater*. 2015;103(4):825–831. doi:10.1002/jbm.b.33262
28. Isobe K, Watanebe T, Kawabata H, et al. Mechanical and degradation properties of advanced platelet-rich fibrin (A-PRF), concentrated growth factors (CGF), and platelet-poor plasma-derived fibrin (PPTF). *Int J Implant Dent*. 2017;3(1):17. doi:10.1186/s40729-017-0081-7
29. Danilatos GD. Review and outline of environmental SEM at present. *J Microsc*. 1991;162(3):391–402. doi:10.1111/j.1365-2818.1991.tb03149.x
30. Inoue N, Takashima Y, Suga M, Suzuki T, Nemoto Y, Takai O. Observation of wet specimens sensitive to evaporation using scanning electron microscopy. *Microscopy (Oxf)*. 2018;67(6):356–366. doi:10.1093/jmicro/dfy041